Summer 6-24-2014

Experimental analysis of air vortex Impingement through porous screens

Xudong An
University of Texas at Dallas

Howard Fultz
University of Texas at Dallas

Fatemeh Hassanipour
University of Texas at Dallas

Proceedings of the 5th International Conference on Porous Media and its Applications in Science and Engineering ICPM5

june 22-27, 2014, Kona, Hawaii, USA

EXPERIMENTAL STUDY OF AIR VORTEX INTERACTION WITH POROUS SCREENS

Xudong An, Howard Fultz, Fatemeh Hassanipour
Department of Mechanical Engineering
University of Texas at Dallas
Richardson, Texas 75080

ABSTRACT

This paper presents the experimental analysis of air flow vortex propagation through porous screens. This study is conducted by a new and unique experimental setup for velocity measurements and visualization of air vortex interaction with porous screen. A custom-made, high-precision vortex generator provides a variety of velocity profiles for vortex generation with an unprecedented level of precision. The flow fields are captured with the use of a fog generator and a high-speed CCD camera. The porous screens are constructed out of acrylic rods with various orientations, thickness, and porosities from rod separation. The results presented in this paper show the effect of porosity and air injection velocity on the behavior of air flow (separation, accumulation), and the transport phenomena of vortex flow while interacting with porous screens.

keywords: porous media, vortex flow

NOMENCLATURE

D	Piston Diameter (m)
Fr	Frame number
Re_J	Jet Reynolds Number
t	time (s)
U	Piston Velocity (m/s)
t_{total}	Total time of air flow (s)
R_P	Piston radius (m)
Δt	Time interval (s)
x, y	Horizontal and vertical axis (m)
ϕ	Surface Porosity

1 INTRODUCTION

A vast number of natural and man-made materials are solids that contain pores for example, rocks, soil, biological tissue, cements, ceramics etc. These porous media are used in many areas of applied science and engineering including filtration, soil mechanics, petroleum engineering, bioengineering etc. The static properties of porous media have been studied intensively for many decades. However, the understanding of dynamic interactions of fluid with porous media remains an important area of investigation that can yield critical and much-needed improvements to applications in health care, environmental and various other areas of engineering.

The study of vortices, their dynamics and various properties is an active and ongoing area of research [1–17].

Olcay and Krueger [18] have investigated turbulent vortex rings to better understand the role of coherent structures in turbulent flow. Bethke and Dalziel [19], and Masuda et al. [20] have studied the collision between vortex ring and particle layers. The dynamic of vortex rings in special types of flow e.g. rotating fluid and cross flows by have also been studied by Yu et al. [21] and Kelso et al. [22] respectively.

The interaction of vortex rings with solid surface has been investigated by Xu et al. [23], Chu et al. [24], Fabris et al. [25], and Gan et al. [26]. Lau and Yu [27] studied the interaction of laminar vortex flow with solid walls to reproduce some of the features observed in turbulent boundary layers. Couch and Krueger [28] studied the impingement of vortex rings with inclined walls. Xu and Feng [29] studied the effects of orifice (vortex ring generator exit) to wall distance on the evolution of vortex structures and flow fields. Yamada et al. [30] investigated the formation and reflection of air vortex flow against flat surface.

Although the subject areas of vortex flow and porous

media have each been individually investigated, few if any results exist in the open literature on the interactions of vortex flows and porous media. The following section outlines these studies with their approaches.

Naaktgeboren [31] studied the interaction of liquid (water) vortex ring with a thin porous screen. They used a piston/cylinder vortex ring generator and the porous screens with porosity between 0.4 and 0.8. They studied the effect of jet Reynolds number (based on piston velocity) and also the ratio of piston stoke to its diameter on vortex ring formation and transmission. They used planar laser-induced fluorescence (PLIF) and digital particle image velocimetry (DPIV) methods for vortex visualization and quantitative measurements.

Adhikari and Lim [32] conducted experimental research to investigate the impact of a vortex ring on solid walls and permeable screens. He studied the effect of Reynolds number and porosity of the screens on the vortex expansion while being impinged on a porous screen.

Hrynuk et al. [33] investigated the interaction of liquid (water) vortex flow with stainless wired mesh porous screens to study the effect of screen wire dimensions on the flow behavior. The porosity of all porous screens were constant (around 0.64), while their wire diameter varied between 0.018 cm (fine mesh) and 0.267cm (coarse mesh). They used Laser Induced Fluorescence (LIF) method to visualize the vortex disruption while passing through the porous screens.

Changing direction from a thin porous media toward the vortex ring propagation inside a cubical porous object,Hassanipour et al. [34] conducted analytical research on the effect of porous medium properties on vortex ring propagation. The effect of porosity, permeability and vortex ring impingement velocity on the flow expansion and contraction in a porous medium was investigated numerically.

The interaction of vortex flow and porous media is on the cutting edge of knowledge in fluid mechanics. Vortex flows are inherently nonlinear and are known to display intriguing behavior while interacting with boundary conditions and various flow conditions. Porous media with their various morphologies are also a challenging area of ongoing study. When these two subject areas come together, an even richer set of conditions emerge and display interesting behaviors.

In this paper the dynamics of air vortex rings is conducted experimentally when colliding with porous screens. A carefully conceived experimental apparatus facilitates precise and repeatable tests involving (dynamic) vortex flows and porous media. To visualize the flow field, the technique of using fog as a fluid marker is selected and a CCD camera captures the flow fields. high-precision vortex generator entirely designed and built in the PI's lab and controlled by a high-speed programmable controller (NI cRIO-9074), the software for which was also developed in-house. The resulting vortex ring formations and their evolution under various impingement velocities are shown. The porous screens are constructed by acrylic transparent rods allowing to visualize and capture the images of the air vortex (fog) propagation through that. The effect of porosity on the transmission of vortex ring though screens are presented. Experimental results show the impact of both porous medium's porosity as well as the jet air Reynolds number on vortex ring flow formation and transport through the porous screens.

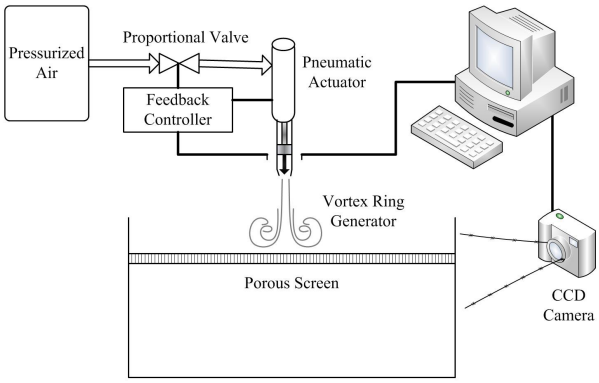

FIGURE 1. Schematic configuration of the experimental setup

2 EXPERIMENTAL SETUP

A schematic of the experimental set up is shown in Figure 1. The air vortex is created by an aluminum piston/cylinder assembly. The cylinder has an outside diameter, inside diameter and length equal to 1.66 in, 1.364 in and 12in respectively. The ejection-side of cylinder was given a slope angle of 7° ending in a sharp rim to minimize flow delamination at the cylinder's edge.

To visualize the flow, a fog generator (Eliminator EF400) was used to fill the cylinder with fog (white). The experiment area was enclosed in black for contrast and to minimize the effect of ambient air flow on the impinged air vortex ring. A 10-Bit black and white CCD Camera (UNIQ, Model UP-685CL) was used to record images of the resulting flow field. The full frame resolution is 659×494 pixels and the camera is capable of capturing 110 frames per second.

A high-speed programmable controller (National Instruments cRIO-9047) was used to command a repeatable trapezoidal velocity profile $u(t)$ for producing precise vortex flow. A pneumatic force actuator with position feedback combined with a proportional valve (both from Enfield Technologies) were used to provide the precise force necessary for the piston to achieve the desired velocity profile. The pneumatic actuator has a built-in linear resistive transducer linked to the piston's position (Fig. 3a). While the wiper glides uniformly along the transducer, the voltage changes linearly, sending the command to the feedback controller. The linear relation between voltage and position that the transducer provides is used to determine the position within 152 nanometers at fully filtered, sub-millisecond sampling rates (Fig. 3b). The solid line represents the com-

manded position velocity profile, where acceleration and deceleration are observed at the top and bottom of the position graph and velocity was constant in central period. The dashed line represents the actual position of the piston, and as seen also in the plot, it responded well to the command. Consecutive positions and the elapsed time reading between these two points are used for determining the actual velocity (Fig. 2). The time intervals can be as small as 10^{-6}s.

The predefined trapezoidal velocity profiles in this study are shown in Equations (1), (2) and (3) with Reynolds numbers Re_J=700, 1800, and 3000 respectively.

$$U(t)(m/s) = \begin{cases} 1.0796t & 0 < t < 0.296 \\ 0.32 & 0.296 \leq t \leq 0.889 \\ -1.0796t + 1.28 & 0.889 \leq t \leq 1.186 \end{cases} \quad (1)$$

$$U(t)(m/s) = \begin{cases} 6.7475t & 0 < t < 0.119 \\ 0.8 & 0.119 \leq t \leq 0.356 \\ -6.7475t + 3.2 & 0.356 \leq t \leq 0.474 \end{cases} \quad (2)$$

$$U(t)(m/s) = \begin{cases} 18.5556t & 0 < t < 0.071 \\ 1.32 & 0.071 \leq t \leq 0.213 \\ -18.5556t + 5.28 & 0.213 \leq t \leq 0.284 \end{cases} \quad (3)$$

Reynolds numbers are calculated based on air properties at room temperature and the maximum piston velocity (U) and diameter of the piston (D).

The high-precision velocity profile controller produced the initial conditions for the given experiment with a high degree of accuracy, thus providing a reliable, repeatability set of experimental data. This high-precision repeatability is particularly desirable for example, when studying the effects of varying porosity and permeability for the same selected velocity profiles (i.e., vortices of different strengths).

The porous screens are made of a transparent wire mesh with total surface area of 50 $\times$ 28 cm and the wire diameter of 0.1cm (Fig. 4). The wire intervals distances are 1 cm, 0.5cm, and 0.25 cm respectively. This results therefore in a screen porosity of $\phi = 0.8$, $\phi = 0.6$ and $\phi = 0.34$, respectively. A pair of acrylic sheet stands support the screen under the piston. The stands were designed in such a way as to allow additional porous screens to easily slide though them horizontally, to enable future studies. The distance between the screen and the exit of the nozzle is around 10cm and is sufficient enough to allow vortex ring evolution to be completed before the ring reaches the bottom of the tank.

3 EXPERIMENTAL RESULTS

To understand the propagation vortex flows through porous screens, a set of experiments were conducted for visualization of free vortex ring formation and progression.

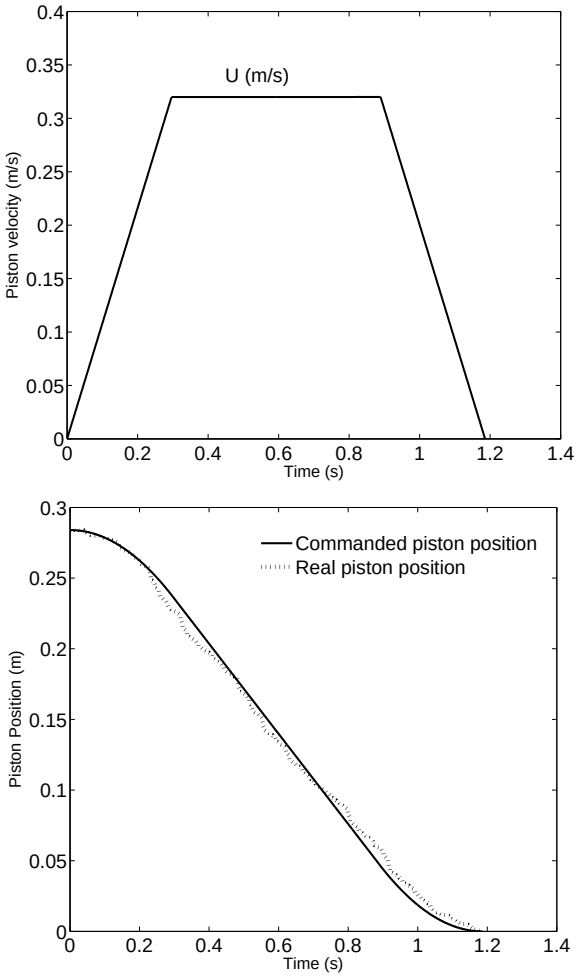

FIGURE 2. A typical trapezoidal velocity profile of piston and the regarding piston position in Labview

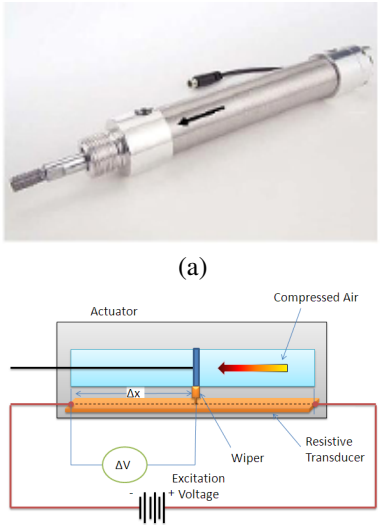

(a)

(b)

FIGURE 3. (a) Pneumatic Actuator and (b) Its position sensing mechanism

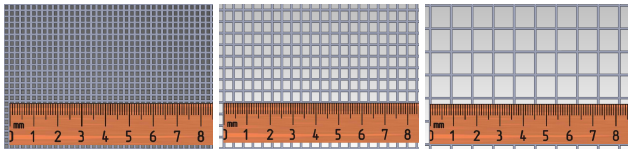

FIGURE 4. Pictures of fine, medium, and coarse wire mesh screens (scale is in the centimeter)

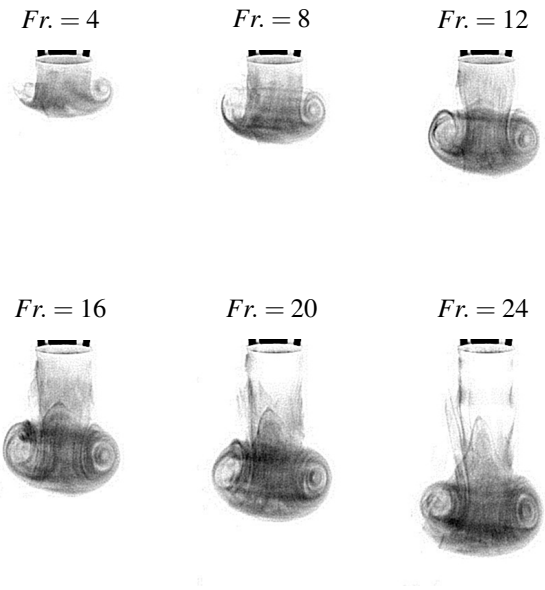

FIGURE 5. Free vortex formation and evolution when Re=1800

Figure 5 illustrates a full vortex ring formation absent the porous media when Re=1800. The vortex ring travels downward symmetrically.

To be able to compare these images in equal time sequences while repeating the test for various Reynolds numbers, the time intervals were manually set on the CCD camera for each Reynolds number based on the capture frame number. The picture capturing moment is shown by *Fr.* which stands for frame number. The time intervals are set in a way that for example at $Fr. = 23$, vortex ring reaches the porous screen regardless of the value of related Reynolds number.

The three sets of time intervals are Δt=0.033, 0.022, and 0.019 seconds for Reynolds numbers 700, 1800, and 3000 respectively. Therefore the total time for each vortex ring ejection from piston stroke all the way to dissipation results in: $t_{total} = 51 \times \Delta t$.

The time frames in Figure 5 are from $Fr. = 4$ (vortex formation immediately after piston ejection) toward $Fr. = 24$ which is the traveling distance between the outlet of the piston and the location of the porous screen. These images are related to free vortex formation and propagation in absence of the porous screen.

The effect of porosity on the flow behavior through the porous medium is shown in Figure 6 for Reynolds number Re=700. The results show that while the vortex ring passes through the screen with large porosity ($\phi = 0.8$), it barely

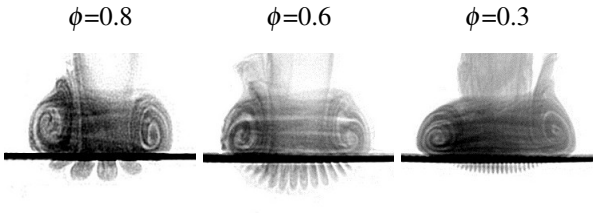

FIGURE 6. Vortex ring interaction with porous screens for Re=700 at *Fr.*=23

passes through the surface with low porosity ($\phi = 0.3$). Decreasing the porosity leads to the formation of secondary vortices which separate from the primary vortex (the one on upstream side of mesh screen) during the interaction. The small amount of transmitted air also tends to reform a new vortex downstream of the porous structure.

For the medium porosity mesh, when the primary vortex ring reaches the porous screen, about half of the impinged air passed through the screen and formed an unclear vortex structure on the other side below. The remainder of primary flow expanded along the mesh until secondary vortices appeared. The high porosity screen showed weak secondary vortex formation. The primary flow mostly passed through the mesh and showed significant distortion downstream. The images in Figure 6 show that the reformation of the vortex ring after passing through the porous surface was a function of its porosity. Primary flow is separated by the wires of the mesh for different wire diameter. Coarse beams are produced when primary vortex interacted with the high porosity screen, while very clean jet-like structures are produced when primary vortex interacted with the low porosity screen.

The three graphs in Figure 7 show the trajectory of vortex flow passing though the screens with various porosities at the same time frame $Fr. = 51$. Due to the symmetric nature of the vortex, only half of the piston and vortex ring is displayed in the graphs (x=0 is center of the piston). The horizontal and vertical axes are shown in dimensionless format and R_P is the radius of the piston. As observed, the air flow expands rapidly as soon it is ejected out of the cylinder ($x/R_P < 2$). After the vortex ring is formed, the expansion in r direction almost stops around ($x < 2.5R_P$) and vortex ring moves downward with an almost constant radius ($x \approx 2.5R_P$). Comparing these graphs shows that for high porosity case, the trajectory of transmitted flow is longer. Also no rolling primary vortex appears upstream of the screen. For the medium and low porosity cases, when primary flow reached the mesh screen, the primary vortex partially crossed through the porous screen while the rest expanded along the mesh surface. The resulting radius of the secondary vortex increases with a decrease in porosity. Also part of the primary vortex expands and keeps rolling further on the surface. In low porosity case, more complicated multiple vortices were observed.

To visualize the effect of Reynolds number on vortex flow behavior while propagating through porous screen, and for constant porosity of ϕ=0.8, three Reynolds number of 700,1800 and 3000 are compared. The trajectory of primary

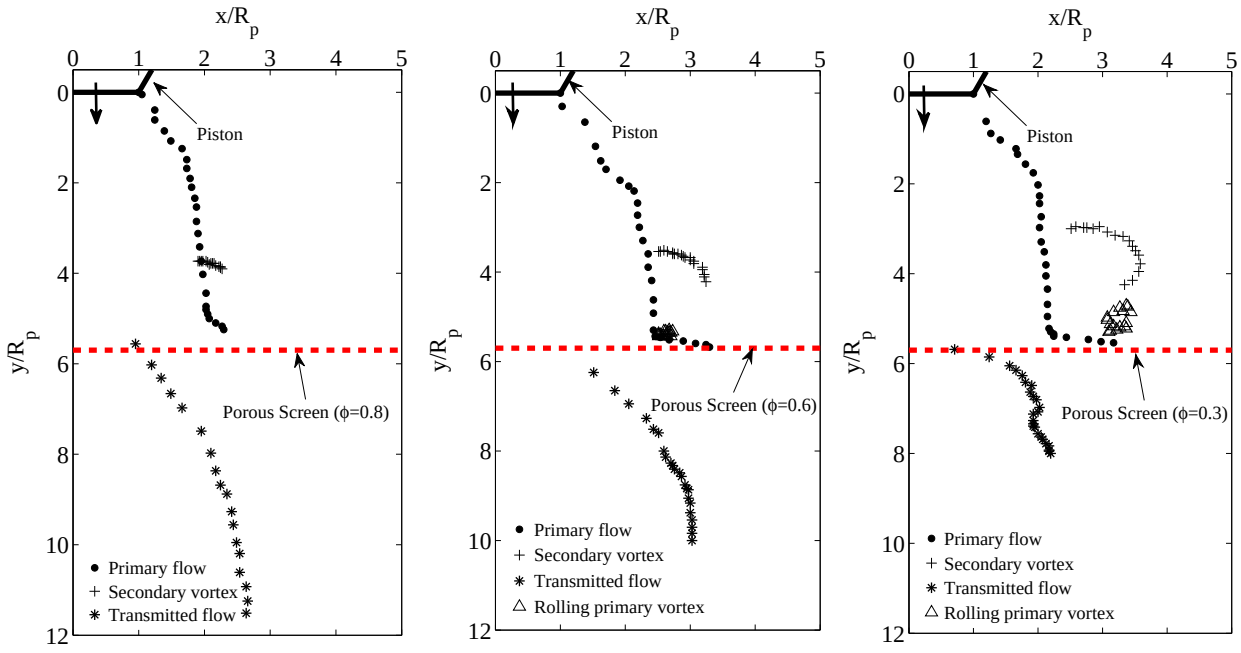

FIGURE 7. Vortex ring interaction with porous screen (Re=700): effect of porosity

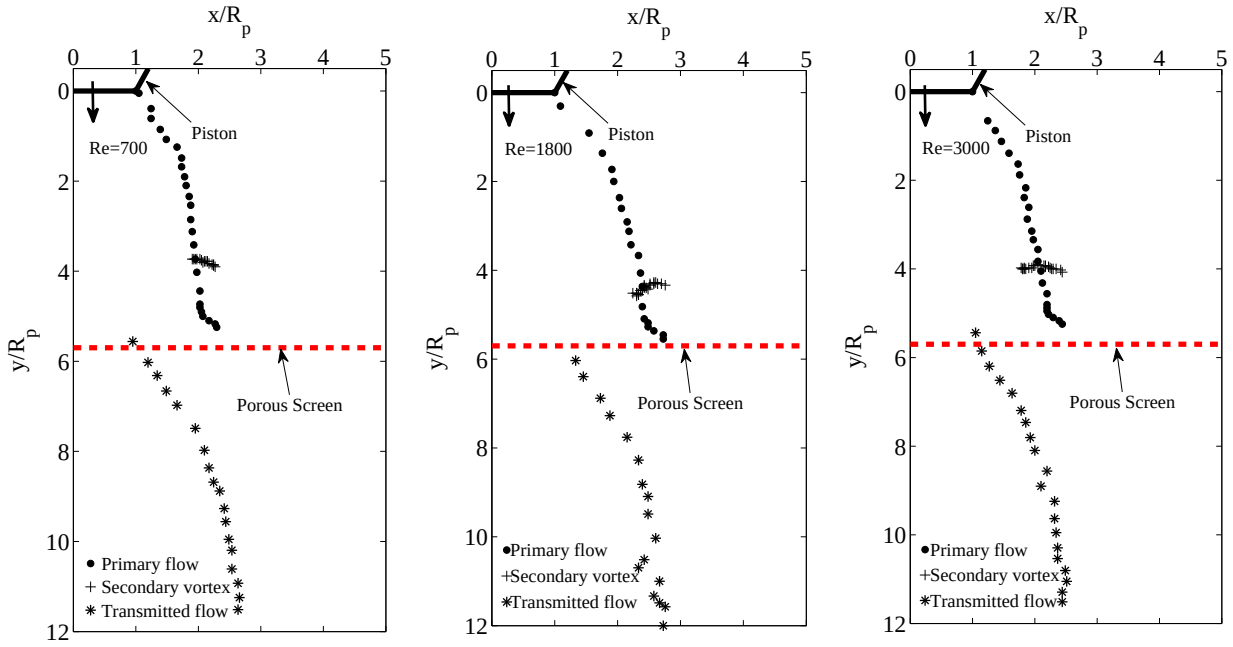

FIGURE 8. Trajectory of vortex ring interaction with porous screen (ϕ=0.8): effect of Reynolds number

vortex, secondary vortex and transmitted flow are shown in figure 8, for which the same results were obtained.

As a summary, the observations reveal that porosity values have dominant affects on the vortex ring expansion, contraction and splitting while interacting the porous screens. The most intriguing behavior of vortices happen while the vortex ring interacts with a fine porous screen.

4 ACKNOWLEDGMENT

The authors acknowledge financial support from the American Chemical Society grant number ACS-PRF-51245 and National Science Foundation (BRIGE) grant number 1227930.

REFERENCES

[1] Maxworthy, T., 1972. "The structure and stability of vortex rings". *Journal of Fluid Mechanics,* **51**, pp. 15–32.

[2] Norbury, J., 1973. "A family of steady vortex rings". *Journal of Fluid Mechanics,* **57**(3), pp. 417–431.

[3] Saffman, P. G., 1978. "The number of waves on unstable vortex rings". *Journal of Fluid Mechanics,* **84**(4), pp. 625–639.

[4] Koschmieder, E. L., 1979. "Turbulent taylor vortex flow". *Journal of Fluid Mechanics,* **93**(3), pp. 515–527.

[5] Cerra, A., and Smith, C., 1983. Experimental observations of vortex ring interaction with the fluid adjacent to a surface. Tech. rep., Interim Report Lehigh Univ., Bethlehem, PA. Dept. of Mechanical Engineering and Mechanics.

[6] Chu, C., and Falco, R., 1987. "Vortex ring/viscous wall layer interaction model of the turbulence production process near walls". *Journal of Experiments in Fluids*, pp. 305–315.

[7] Glezer, A., 1988. "The formation of vortex rings". *Physics of Fluids,* **31**.

[8] Glezer, A., and Coles, D., 1990. "An experimental study of a turbulent vortex ring". *Journal of Fluid Mechanics,* **211**, pp. 243–283.

[9] Chang, Y. K., and Vakili, A. D., 1995. "Dynamics of vortex rings in crossflow". *Physics of Fluids,* **7**, p. 1583.

[10] Verzicco, R., Orlandi, P., Eisenga, A., van Heijst, G. J. F., and Carnevale, G. F., 1996. "Dynamics of a vortex ring in a rotating fluid". *Journal of Fluid Mechanics,* **317**, pp. 215–239.

[11] James, S., and Madnia, C., 1996. "Direct numerical simulation of laminar vortex ring". *Physics of Fluids,* **8**(9), p. 2400.

[12] Barenghi, C. F., and Samuels, D. C., 1997. "Superfluid vortex lines in a model of turbulent flow". *Physics of fluids,* **9**.

[13] Lim, T., 1998. "On the breakdown of vortex rings from inclined nozzles". *Physics of Fluids,* **1**(7), pp. 1666–1671.

[14] Gharib, M., Rambod, E., and Shariff, K., 1998. "A universal time scale for vortex ring formation". *Journal of Fluid Mechanics,* **360**(121-140), p. 394.

[15] Kim, T., Hodson, H., and Lub, T., 2005. "Contribution of vortex structures and flow separation to local and overall pressure and heat transfer characteristics in an ultralightweight lattice material". *International Journal of Heat and Mass Transfer,* **48**(19-20), pp. 4243–4264.

[16] Jiang, Houshuo, and Grosenbaugh, M. A., 2006. "Numerical simulation of vortex ring formation in the presence of background flow with implications for squid propulsion". *Theoretical and Computational Fluid Dynamics,* **20**(2), pp. 103–123.

[17] Liu, C. H., 2002. "Vortex simulation of unsteady shear flow induced by a vortex ring". *Computers and Fluids,* **31**(2), pp. 183–207.

[18] Olcay, A., and Krueger, P., 2007. "Measurement of ambient fluid entrainment during laminar vortex ring formation". *Journal of Experiments in Fluids*, pp. 235–247.

[19] Bethke, N., and Dalziel, S., 2012. "Resuspension onset and crater erosion by a vortex ring interacting with a particle layer". *Physics of Fluids,* **24**, p. 063301.

[20] Masuda, N., Yoshida, J., Ito, B., Furuya, T., and Sano, O., 2012. "Collision of a vortex ring on granular material. part i. interaction of the vortex ring with the granular layer". *Fluid Dynamics Research,* **44**(1), p. 015501.

[21] Yu, P., Lee, T. S., Zeng, Y., and Low, H. T., 2008. "Vortex breakdown in an enclosed cylinder with a partially rotating bottom-wall". *Journal of Fluids Engineering,* **130**(11), p. 111101.

[22] Kelso, R. M., Lim, T., and Perry, A., 1996. "An experimental study of round jets in cross-flow". *Journal of Fluid Mechanics,* **306**(1), pp. 111–144.

[23] Xu, Y., Feng, L.-H., and Wang, J.-J., 2013. "Experimental investigation of a synthetic jet impinging on a fixed wall". *Experiments in Fluids,* **54**(5), pp. 1–13.

[24] Chu, C.-C., Wang, C.-T., and Chang, C.-C., 1995. "A vortex ring impinging on a solid plane surfacevortex structure and surface force". *Physics of Fluids,* **7**, p. 1391.

[25] Fabris, D., Liepmann, D., and Marcus, D., 1996. "Quantitative experimental and numerical investigation of a vortex ring impinging on a wall". *Physics of Fluids,* **8**, p. 2640.

[26] Gan, L., Nickels, T., and Dawson, J., 2011. "An experimental study of a turbulent vortex ring: a three-dimensional representation". *Experiments in fluids,* **51**(6), pp. 1493–1507.

[27] Lau, J., and Fisher, M., 2006. "The vortex-street structure of turbulent jets". *Journal of Fluid Mechanics Digital Archive*, pp. 299–337.

[28] Couch, L. D., and Krueger, P. S., 2011. "Experimental investigation of vortex rings impinging on inclined surfaces". *Experiments in fluids,* **51**(4), pp. 1123–1138.

[29] Xu, Y., and Feng, L., 2013. "Influence of orifice-to-wall distance on synthetic jet vortex rings impinging on a fixed wall". *Science China Technological Sciences*, pp. 1–9.

[30] Yamada, H., Kohsaka, T., Yamabe, H., and MATSUI, T., 1982. "Flowfield produced by a vortex ring near a plane wall". *Physical Society of Japan, Journal,* **51**, pp. 1663–1670.

[31] Naaktgeboren, C., 2007. "Interaction of pressure and momentum driven flows with thin porous media: Experiments and modeling".

[32] Adhikari, D., and Lim, T., 2009. "The impact of a vortex ring on a porous screen". *Fluid Dynamics Research,* **41**(5), p. 051404.

[33] Hrynuk, J. T., Van Luipen, J., and Bohl, D., 2012. "Flow visualization of a vortex ring interaction with porous surfaces". *Physics of Fluids,* **24**, p. 037103.

[34] Hassanipour, F., Raya, I. P., and Mortazavi, S. N., 2013. "Simulation of vortex ring permeation in porous media". *Journal of Porous Media,* **16**(7).